Theor Appl Climatol (2015) 119:539–550
DOI 10.1007/s00704-014-1128-9

ORIGINAL PAPER

Study on the reliable computation time of the numerical model using the sliding temporal correlation method

Yong Liu · Pengfei Wang · Gang Huang

Received: 7 October 2013 / Accepted: 9 February 2014 / Published online: 5 March 2014

Abstract A simple and useful method, the sliding temporal correlation (STC) analysis, is employed in the present work to investigate the predictable time (PT) of two typical chaotic numerical models (Lorenz system and Chen chaotic system) and reliable computing times (RCT) of an atmospheric general circulation model (ECHAM5). Through kinds of numerical experiments, results indicate that the maximal prediction time of Lorenz system (and Chen chaotic system) detected by STC method is coherent well with that by classical error limitation method, suggesting the effective role of the STC method. Then, taking the geopotential height for example, the RCT of ECHAM5 and potential impact factors such as the integration time step, initial condition, and model's resolution are explored. Results reveal that (1) the high-value areas of the RCT are mainly situated in the tropics, and the global mean RCT (GMRCT) decreases from with the time step increasing; (2) the ocean forcing can enlarge the difference of the RCT between that averaged over the Southern Hemisphere (SH) and Northern Hemisphere (NH), which implies the RCT in the NH may be more sensitive to the computation error than that in the SH; (3) the model's RCT also displays significant seasonality having longer (about 1–2 days) GMRCT in the experiment integrating from winter than that from summer; (4) the RCT of the high-resolution (T106) ECHAM5 shows similar spatial feature to that of low-resolution (T63) ECHAM5, but the GMRCT and hemispheric difference decreases.

Y. Liu · P. Wang
Center for Monsoon System Research, Institute of Atmospheric Physics (IAP), Chinese Academy of Sciences (CAS), Beijing 100190, China

P. Wang (✉) · G. Huang
State Key Laboratory of Numerical Modeling for Atmopsheric Sciences and Geophysical Fluid Dynamics, IAP, CAS, Beijing 100029, China
e-mail: wpf@mail.iap.ac.cn

G. Huang
Collaborative Innovation Center on Forecast and Evaluation of Meteorological Disasters, Nanjing University of Information Science & Technology, Nanjing 210044, China

1 Introduction

The predictable time (PT) or reliable computing time (RCT) of a numerical model can be simply defined as the specific moment when the error of the numerical model, which increases gradually during the numerical calculation because of the algorithm truncation error and float-point round-off error, reaches the prescribed threshold. Previous studies documented that some nonlinear systems still have the RCT due to the round-off error even they have perfect initial values (Li et al. 2000; Teixeira et al. 2007; Liao 2009). For instance, they pointed out that the Lorenz system (LEs) has a PT with value of about 35 time units (TU) under double precision computation. As for a more complex numerical model, such as the atmospheric general circulation model (AGCM) and the weather forecast model, both the initial values and algorithm/rounding errors can influence the model's RCT and further constraint the model's prediction/simulation capability. Thus, the RCT of the numerical model is not only a mathematical issue but also an essential factor to evaluate the model's performance, which is of great importance and worth investigation. Despite that several studies focused on the computability of the numerical model (Wang et al. 2009; Song et al. 2012), the specific RCT of such kind of model (AGCM or weather forecast model) and the method to estimate the model's RCT are still not well understood, which calls for further study.

The PT/RCT of one numerical model is close related to the PT/RCT of its dynamic system as well as the error growth law. The Lyapunov exponent is one common method to describe the average growth rate of the initial error of one chaotic system, which is widely adopted to explore the characteristic of the chaotic dynamic system (Oseledec 1968). As for a chaotic system, if its initial error is δ_0 and allowed maximal error is Δ (referred as error limitation), then the predictability limit of the chaotic system is defined as $T_p \sim \frac{1}{\lambda_{\max}} \ln\left(\frac{\Delta}{\delta_0}\right)$, among which $\lambda_{\max}$ is the maximum Lyapunov exponent (Eckmann and Ruelle 1985; Wolf et al. 1985; Lorenz 1996). After that, the Lyapunov exponent is extended to the local Lyapunov exponent (Yoden and Nomura 1993) and nonlinear local Lyapunov exponents (NLLE) (Ding and Li 2007a, b; Ding and Li 2012; Li and Ding 2011), which are employed to study the local dynamical feature of the chaotic system. Moreover, the NLLE is a newly developed method that employs the primitive equation to estimate the average error growth rate and error saturation property and can be used to the investigated the predictability of the real weather and climate system.

The error limitation (Δ) is an approach to reveal the RCT / PT which is used in both the linear and nonlinear Lyapunov exponent methods. For convenience, we usually utilize the error growth curve rather than the Lyapunov exponent to estimate the RCT /PT of the dynamic system. At first, we obtain the error growth curve through numerical experiment or other methods, then figure out the first moment when the error δ ($\delta_0 < \Delta$) reaches Δ, namely the RCT/PT. As for different dynamic systems, the choice of appropriate Δ often depends on the true solutions. To avoid this dependency of Δ, the relative error approach was adopted in some studies (Li et al. 2000; Wang et al. 2006; Liao 2009; Liao and Wang 2014). For example, Liao (2009) applied the relative error 5 % Δ and introduced another limit $u_1 u_2 < -\varepsilon$ ($\varepsilon > 0, u_1$ and u_2 denote the trend of different solutions to one variable) to qualify the RCT/PT. The criteria for the NLLE to study the RCT are more complex. Concerning a nonlinear dynamic system, we often choose $\Delta = 95\ \%\overline{E}$ ($\overline{E}$ is the saturation error). Before we get the RCT/PT, we need to calculate $\overline{E}$ first, however, the calculation of $\overline{E}$ needs enough samples and is rather time-consuming.

The error limitation methods mentioned above can be applied to the investigation of RCT/PT on both the whole and the local or individual variable of one dynamic system. Besides, for a less δ_0, numerical experiment and theoretical analysis results confirmed that the RCTs of a dynamic system based on the methods mentioned above showed similar results, and the RCT/PTs of individual variable and the whole system are very close. In view of the limitation of the above methods, such as time-consuming and system dependency, in

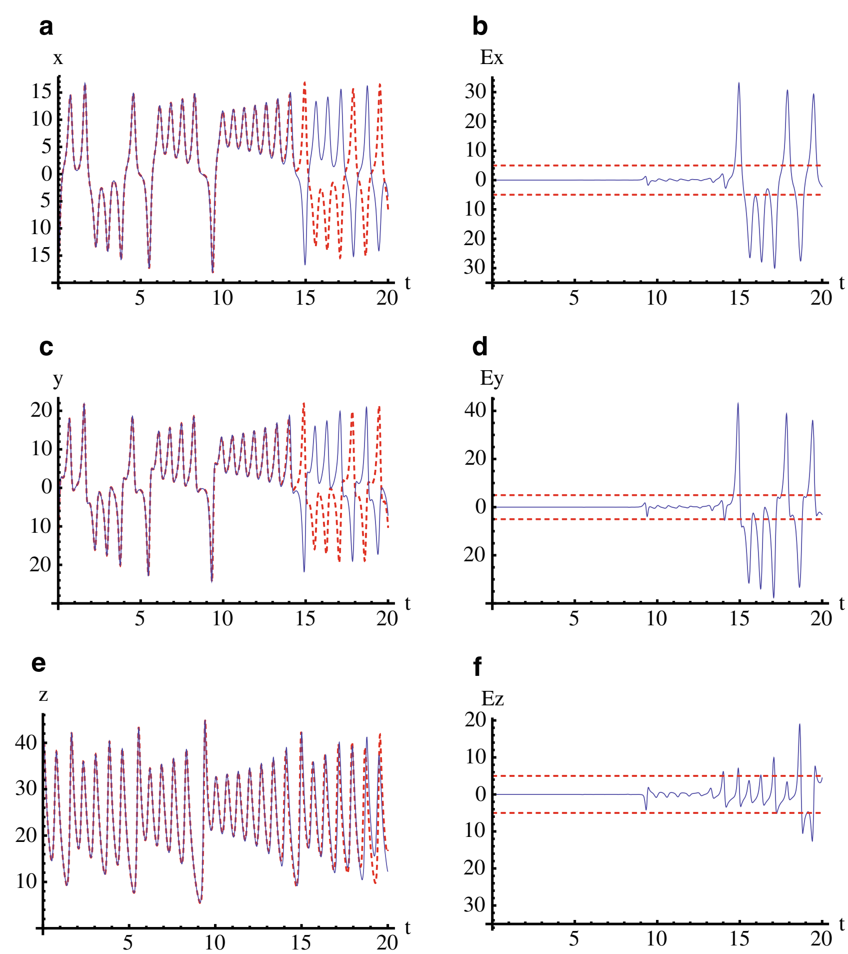

Fig. 1 The evolutions of the solutions and solution errors of the Lorenz system based on the reference and error initial value, and the solution error is defined as the difference between the reference solution and error solution. **a**, **c**, and **e** is solutions for x,y,z, respectively. The solid *blue* (*dotted red*) *lines* in **a**, **c**, and **e** exhibit reference (error) solution. **b**, **d**, and **f** is the solution errors (*solid blue line*) for x,y,z, respectively, among which the *red line* is the error limitation Δ (here, $\Delta = \pm 5$)

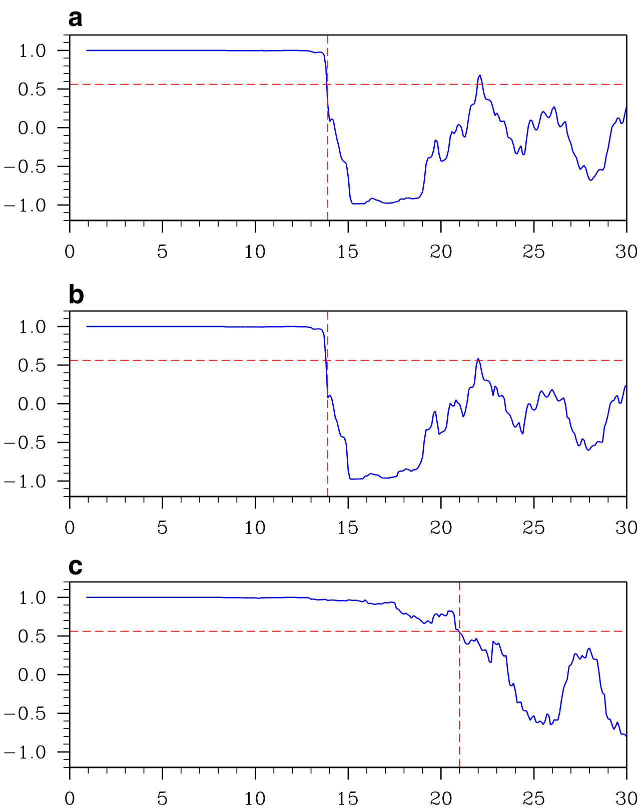

Fig. 2 The evolution of the STC between the reference and error solutions. **a** *x*, **b** *y*, and **c** *z*. The *horizontal dotted line* denotes the reference value corresponding to the 99 % confidence level, and the *vertical dotted line* denotes the first time when the STC reaches the reference value

this study, we present a simple and useful method, the sliding temporal correlation (STC), to study the RCT/PT of the dynamic system and the complex AGCM; the introduction and the advantage of the STC method will be given in the following sections.

2 Methodology

The correlation analysis method is a common method that is widely employed to investigate the relationship between two samples, no matter whether the two samples are linear or nonlinear systems. The STC is based on the common correlation method and supposing a sliding window and often applied to study the variation of the relationship between two time series. The significance of the relationship between the two time series can be tested by the two-tailed Student's *t* test, and for a given confidence level, such as 99 %, the transition time or time span of their relationship can be achieved based on the evolution of the STC.

Generally, the STC is applied to study the relationship between two different time series or two different dynamic systems. While, if we apply it to two similar time series *x*, *y*, and *y* is same as *x* but with initial error, the STC can be considered as the linkage between the error time series and the reference time series, which further can be utilized to investigate the RCT. In addition, we introduce a limit that

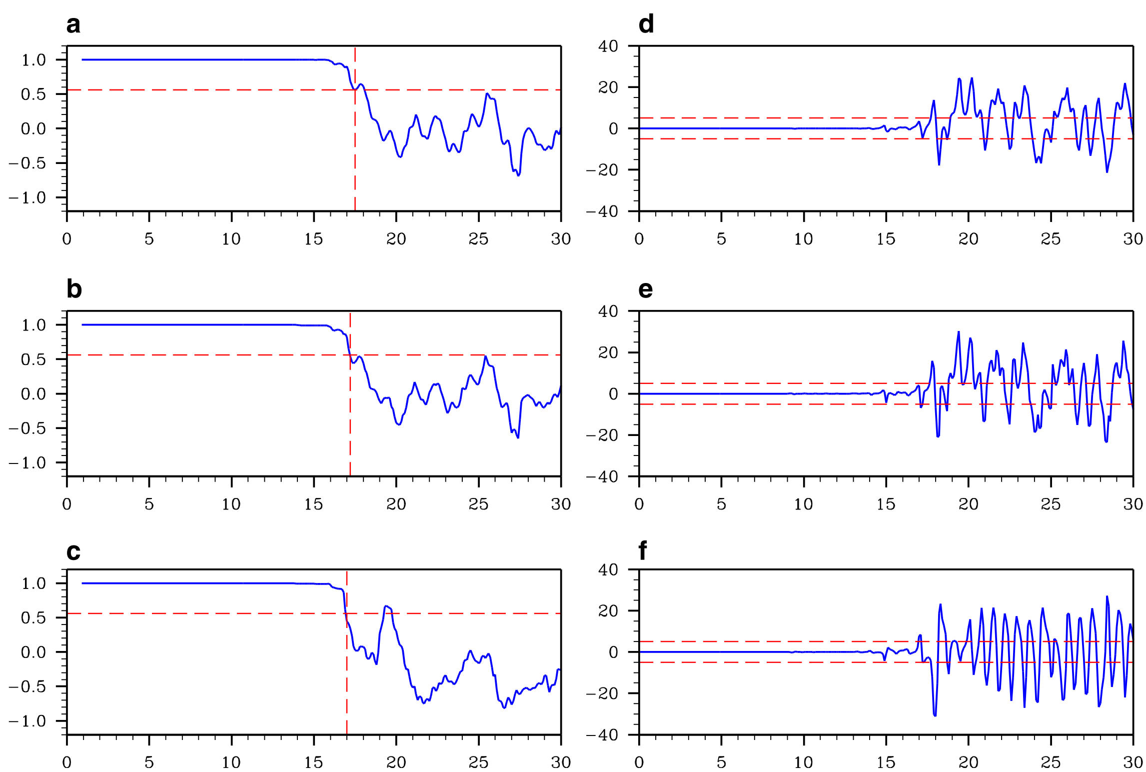

Fig. 3 The STC and solution error based on the experiment with initial error $\delta_0 = 10^{-6}$. **a–c** is same as Fig. 2a–c and d–f display the solution error same as Fig. 1b, d, f

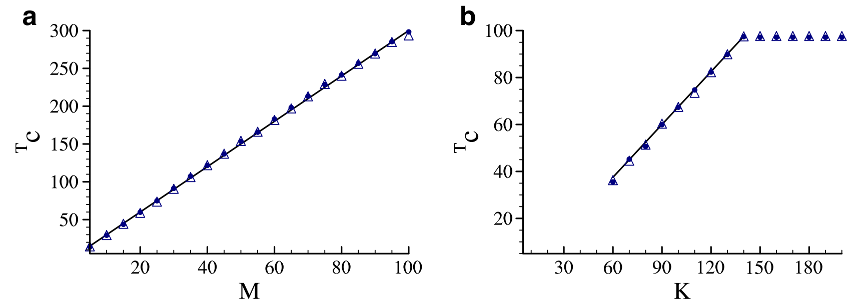

Fig. 4 **a**. The T_c-M diagram for Lorenz system with K=666, and the *line* is T_c=3M. **b**. The T_c-K diagram for Lorenz system with M=32 and the *line* is T_c=0.75K−7.5. The precision here is binary bits. The *triangle* (*dotted*) denotes the results of error limitation (STC) method

the initial error is relative small and the correlation between reference time series and the error time series close to one; and when the error saturates, the correlation gets close to zero. While, as the limitation of number of the sample and the sliding window we select to compute the STC, the first time when the STC beyond the confidence level is defined as the RCT. These criteria are suitable for common numerical models. And on contrast to the error limitation, the STC shows several advantages: (1) it can be applied to study the RTC of the linear and nonlinear dynamical system; (2) it avoids the mistake of the RCT caused by the severe disturbance of the error when using the error limitation method; (3) it is not necessary to use the absolute error, to estimate the solution domain and get the saturation error in before.

Hereafter, we will employ the STC method to study its validity in detecting the RCT/PT of the dynamic systems. Firstly, we examine the PT of the common chaotic dynamic systems by using both the STC and the error limitation methods, and then the STC is adopted to explore the RCT/PT of one climate numerical model. It should be noted that the STC mentioned below denotes the correlation between two samples from similar numerical model results but with the initial error (or with same initial value, but different parameters such as different time step, initial condition, and so on).

3 The predictable time (PT) of the chaotic dynamical systems

In this section, the common chaotic systems, Lorenz system and Chen system, are selected as examples, and the STC and error limitation methods are used to detect their PTs.

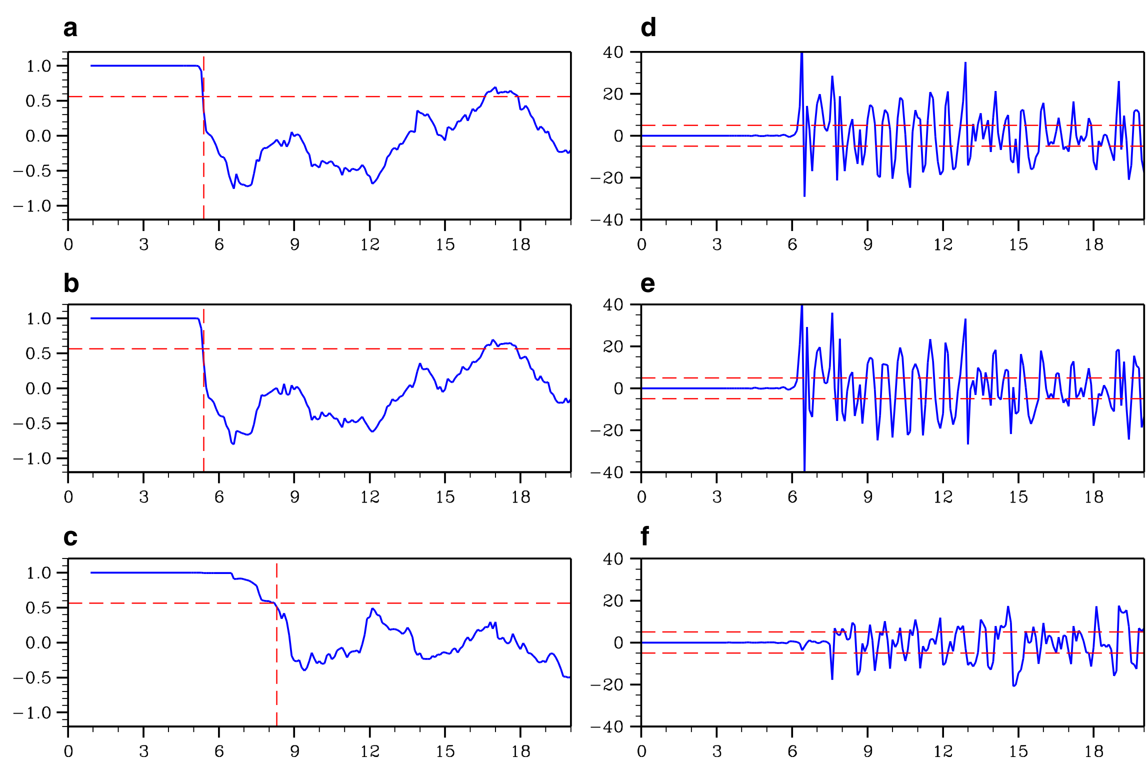

Fig. 5 Same as Fig. 3 but for Chen system with initial error δ_0=10^{-5}

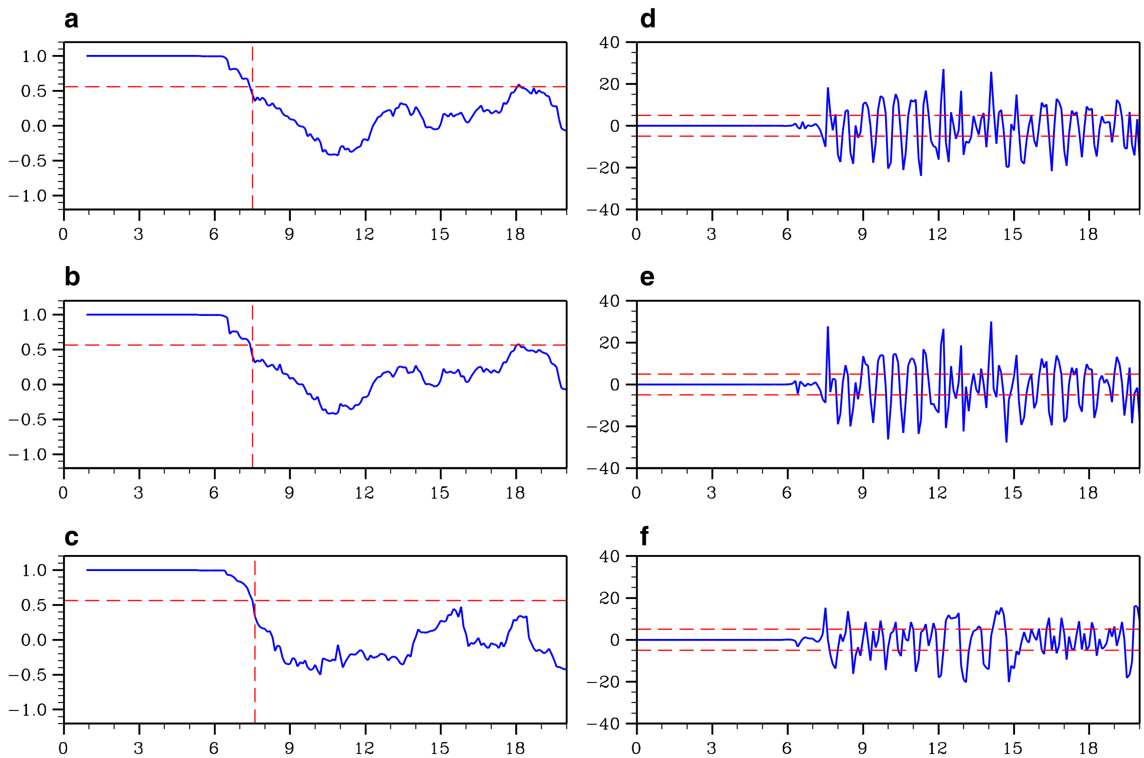

Fig. 6 Same as Fig. 5 but for initial error δ_0=10^{-6}

3.1 Lorenz system

The Eq. 1 shows the Lorenz system (Lorenz 1963), among which σ, r, b are nondimensional constants with values *28.0, 10.0,* and *8/3*, respectively, and t is nondimensional time (unit: TU). As for the Lorenz system, three numerical experiments with different initial values are conducted which aims to get the reference solution and error solution. The reference initial values of x_0, y_0, z_0 are *−15.8, −17.48*, and *35.64,* respectively, and the other two error initial values of x_0, y_0, z_0 are similar as the reference ones but with less disturbance δ_0=10^{-5} and δ_0=10^{-6} plus on the x_0, y_0, z_0, respectively.

$$\begin{cases} \frac{dx}{dt} = -\sigma x + \sigma y \\ \frac{dy}{dt} = rx - y - xz \\ \frac{dz}{dt} = xy - bz \end{cases} \tag{1}$$

Based on the theory of error limitation, the predictability limit of the chaotic system is defined as $T_p \sim \frac{1}{\lambda_{\max}} \ln\left(\frac{\Delta}{\delta_0}\right)$, the PT here is about $\frac{1}{0.906} \ln\left(\frac{5}{10^{-5}}\right) = 14.5$ TU. As for the experimental results, the evolutions of the reference and error solutions and their differences for x,y,z are plotted in Fig. 1. The reference solution and error solution for x in Fig. 1a–b show a very little difference prior to about 15 TU and notable difference since then, and corresponding to the Δ=±5 in Fig.1b, the experiment result indicates that the PT for x is 14.7 TU. The features of the reference and error solutions for the y resemble those for x, and the PT revealed by the experiment is 14.1 TU. As for the variable z, the spread between reference and error solution is not as significant as the variables x, y, and from the error time series in Fig. 1f, we can obtain the PT for z is 13.9 TU. The PT of each variable from numerical experiments results is consistent with the overall PT of the Lorenz system

Fig. 7 Same as Fig. 4 but for the Chen System

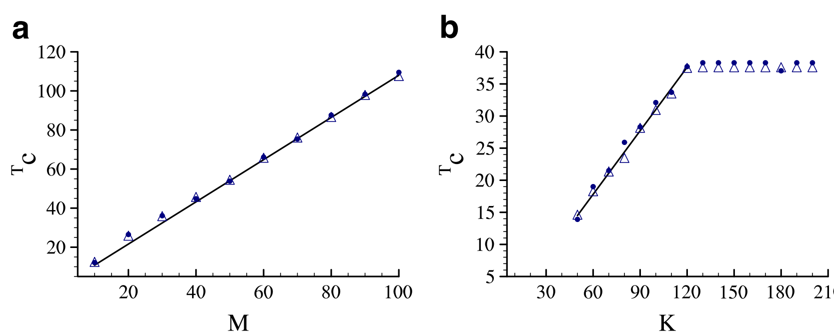

from the theoretical analysis, and the overall PT from the numerical experiment can also be achieved which is close to the PT based on theoretical analysis (figures not shown).

Now, we employ the STC method to study the PT of the Lorenz system based on numerical results of the reference and error solutions. Here, the sliding window is defined as 20 time intervals (one time interval is 0.1 TU), i.e., 2 TU. Figure 2 shows the evolutions of the STC between the reference and error solution for x,y,z, respectively. We can see the PTs for x,y,z are 13.9 TU, 13.9 TU, and 21.0 TU, respectively, based on the 99 % Student's t test. The PTs of variables x,y are very close to the theoretical analysis (14.5 TU) and Δ detection (14.7 TU, 14.1 TU). However, the PT tested from STC is quite different from that from theoretical analysis and Δ detection. As can be seen in Figs. 1e and 2c, the reference and error solution of z show similar evolution feature and the STC changes slowly, therefore, the statistical PT is longer. Since the Δ detection method is from the dynamical respect to get the PT, and the STC is a statistical method that calls for multisamples of numerical experiments to get the PT, thus the PT from single experiment which is different from the theoretical and Δ method is acceptable.

Another similar experiment is also made based on the initial error $\delta_0=10^{-6}$, corresponding to which the theoretical PT is about 17.0 TU. The STCs and differences between reference solution and error solution are shown in Fig. 3. The PTs for x,y,z detected by STC method are 17.5 TU, 17.2 TU, and 17.0 TU, respectively, (Figs. 3a–c), and those by error limitation Δ method are 17.7 TU, 17.1 TU, and 16.9 TU, respectively (Figs. 3d–f). Both of them match well with the theoretical results.

Since its ability to reveal the evolution of the correlation between two time series, the STC method can also be employed to detect the RCT of a dynamic system caused by numerical error. For example, Liao (2009) applied clean numerical simulation method with 400 orders Taylor series and 800 significant digits mathematical program to obtain the 1,200 TU result. Moreover, Liao (2009) propose the experimental way to obtain the relation between the order of Taylor methods (M) and T_c (the reliable computation time sometimes be called as critical computation time, and we abbreviate it as T_c). Since this type of computation have no initial error δ_0, thus we can regard it as a different issue with predictability of initial error problem. But the determination of error approaching to error limitation is similar, so when we study T_c, we can still use the $\Delta=5$ as error limitation criterion. The numerical algorithms to study T_c can be found in Liao (2009) and Wang et al. (2006, 2012). By applying this method, we first keep the precision, for example, $K=666$ and change the order from $M=20-100$ (interval with 10), then we could obtain each T_c according to M and we call it as T_c-M diagram. Secondly, we keep the order be constant such as $M=32$ and make the precision various $K=50-200$ (interval 10) to obtain the T_c-K diagram.

Table 1 The vertical and horizontal resolution and related default time step of the ECHAM5

	T31	T42	T63	T85	T106	T159	T213	T255	T319
L19	2,400	1,800	1,200	900	720	–	–	–	–
L31	1,800	1,200	720	480	360	240	180	150	150
L39	900	900	600	450	360	240	180	150	120

The result indicates that the STC can obtain the correct T_c-M and T_c-K diagrams as well as the error limitation ($\Delta=5$) method (Fig. 4). The correct T_c-M and T_c-K diagrams are fundamental to analyse the computation parameter to obtain the reliable computation time result in $[0,T_c]$, and these parameters instruct the long time simulation of Lorenz system.

3.2 Chen system

Chen and Ueta (1999) documented another chaotic system depicted in Eq. 2, among which $a=35, b=3, c=28$. Like that in Section 3.1, we conducted three experiments to get the (x,y,z) solutions including one reference experiment with initial values $(x_0,y_0,z_0)=(-3,2,20)$ and two contrast experiments having initial values as that in the reference one but with errors $\delta_0=10^{-5}$ and $\delta_0=10^{-6}$ plus on them, respectively.

$$\begin{cases} \frac{dx}{dt} = -ax + ay \\ \frac{dy}{dt} = (c-a)x + cy - xz \\ \frac{dz}{dt} = xy - bz \end{cases} \tag{2}$$

The STC and error limitation methods are applied to study the predictable time (PT) of Chen system. As for the contrast experiment with initial error $\delta_0=10^{-5}$ (Fig. 5), the PTs for (x,y,z) detected by STC (Fig. 5a–c) method are 5.3 TU, 5.3 TU, and 8.3 TU, respectively, and those by error limitation method are 6.2 TU, 6.1 TU, and 7.6 TU, respectively. The discrepancies are within 1 TU. When the initial error is $\delta_0=10^{-6}$ (Fig. 6), the PTs for (x,y,z) detected by the two methods are

Table 2 The description of the experiments

Number	Name	Description
1	AMIP	Forcing by the varied SST, integrated from 1978.1.1 to 1978.6.30
2	CTL	Same as AMIP experiment but without SST forcing,
3	CTL-JJA	Same as CTL experiment but integrated from1978.7.1 to 1978.12.31
4	CTL-T106	Same as CTL but based on the high resolution version T106

very close, and those by STC method are 7.5 TU, 7.5 TU, and 7.6 TU, respectively (Fig. 6a–c) and those by error limitation method are 7.5 TU, 7.5 TU, and 7.5 TU, respectively. Besides, the PTs detected by the two methods become closer as the initial error decreases. From Figs. 3 and 6, we can see that the PTs for the Lorenz system are longer than those for Chen system; this is because the Lyapunov exponent for Lorenz system is larger than that for Chen system.

The result in Fig. 7 indicates that the STC can obtain the correct T_c-M and T_c-K diagrams as well as the error limitation (Δ=5) method for Chen system.

4 The RCT of one AGCM (ECHAM5)

The results revealed in Section 3 indicated the capability of the STC method in studying the PT and RCT for the typical chaotic system. Moreover, the STC method is simple, easy computing, and not subject to the system property (linear or nonlinear). In this section, we employ it to discuss the RCT of one AGCM.

4.1 Model and experiment design

The AGCM ECHAM5 is adopted in this study, which is supplied by the Max Planck Institute for Meteorology, the detailed introduction can be found in Roeckner (2003). The ECHAM5 is a distinguished model that is utilized in the many international model comparison projects such as IPCC AR3, AR4, and AR5. And it is considered to be one of the excellent models in the world and is widely used in the climate research.

It is a spectral model and provides kinds of choice in the vertical and horizontal resolutions. Corresponding to each resolution, there is a specific integration time step (in Table 1). As for this kind of complex climate model, the order in the spatial-temporal integration is fixed, which is not easily

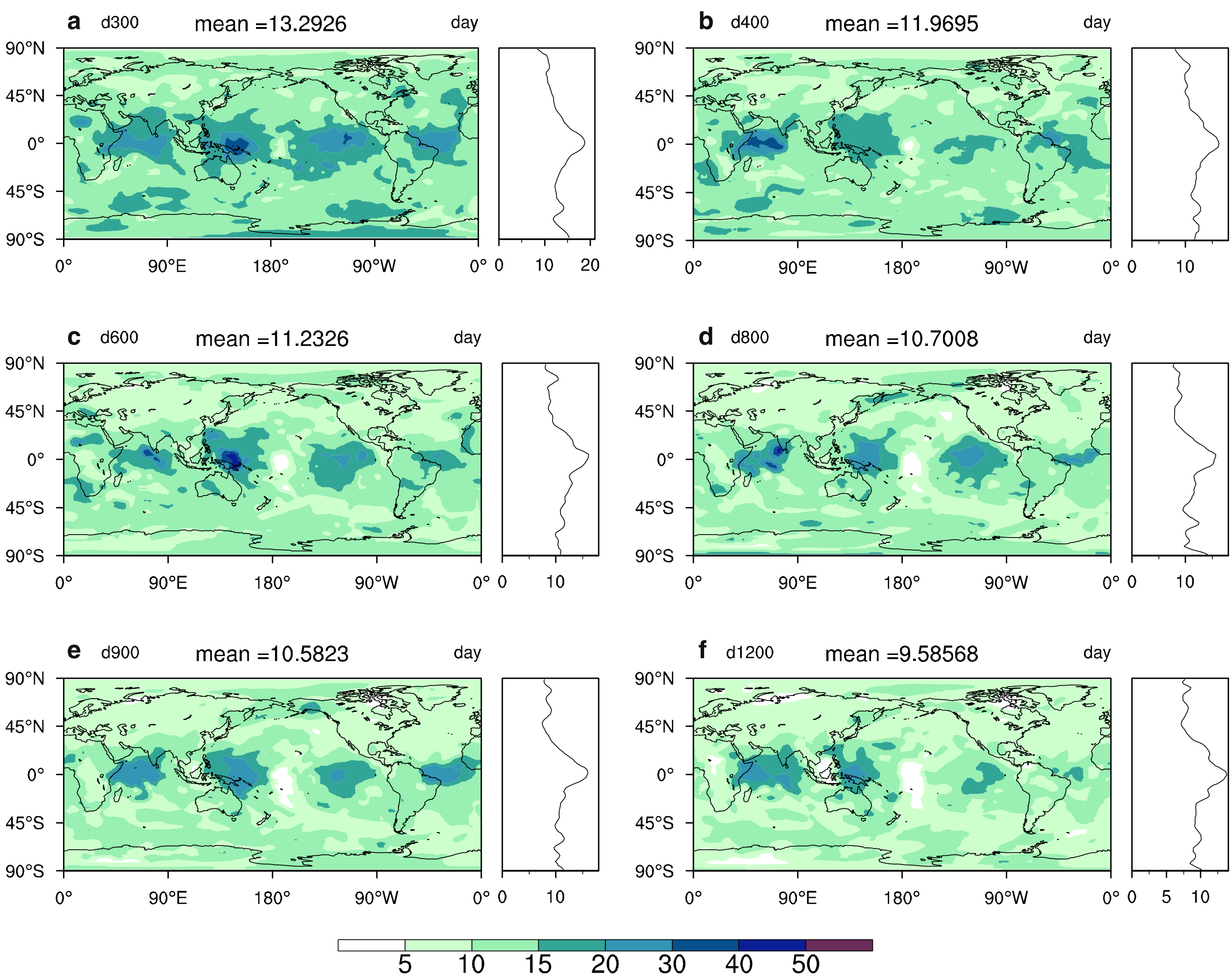

Fig. 8 The spatial distribution of the RCTs (unit: day) of the 500 hPa geopotential height (*shaded*) and their zonal mean (*line*) based on the AMIP experiment with different time steps. (**a**) 300 s, (**b**) 400 s, (**c**) 600 s, (**d**) 800, (**e**) 900 s, and (**f**) 1,200 s. The value in the *center* of each subpanel denotes the global mean of the RCTs

modified. Whereas, the integration time step is an operational way to study the RCT of the model. In addition, the ECHAM5 model provides a parameter *delta_time* to facilitate users to choose the integration time step. In view of the computing resources, we chose the model resolution of T63L19, seven experiments are made with integration time steps as 200, 300, 400, 600, 800, 900, and 1,200, and the experiment with time step 200 denotes the reference time step. The model is integrated from 1978.1.1~1978.6.30, and the outputs with interval 6 h are used in this study. Each of the above seven experiments consists of two set experiments which are related to with/without sea surface temperature (SST) forcing separately. The two set experiments are named as the control run (the sea surface temperature (SST) is fixed, named as CTL) and the SST forcing run (named as AMIP). In order to investigate the initial condition (the start time of the model integration) and the model resolution impacts on the RCT, two additional experiments are conducted. One is similar to the CTL run but with the model integration from 1978.7.1~1978.12.31 (named as CTL-JJA), another one is like CTL run but with a high model resolution T106L19 (named as CTL-T106). The experiments description is shown in Table 2.

As mentioned above, for one variable from the experiments of same kind, each time series has the same initial value, and then the time series may vary differently under the dynamical system control because of different time steps, forcing, and resolutions. Therefore, we take the variable geopotential height as an example to study the RCT of the ECHAM5. Here, we use the 6-h geopotential height outputs, the sliding window with value 20, and the 99 % confidence level based on Student's *t* test. And the spatial distribution of the RCT of the ECHAM5 is concerned in this section.

4.2 The RCT of the model

Figure 8 displays the spatial distributions of the RCT of the 500 hPha geopotential height based on the AMIP experiment, which reflects the RCT of the model with the SST forcing. It

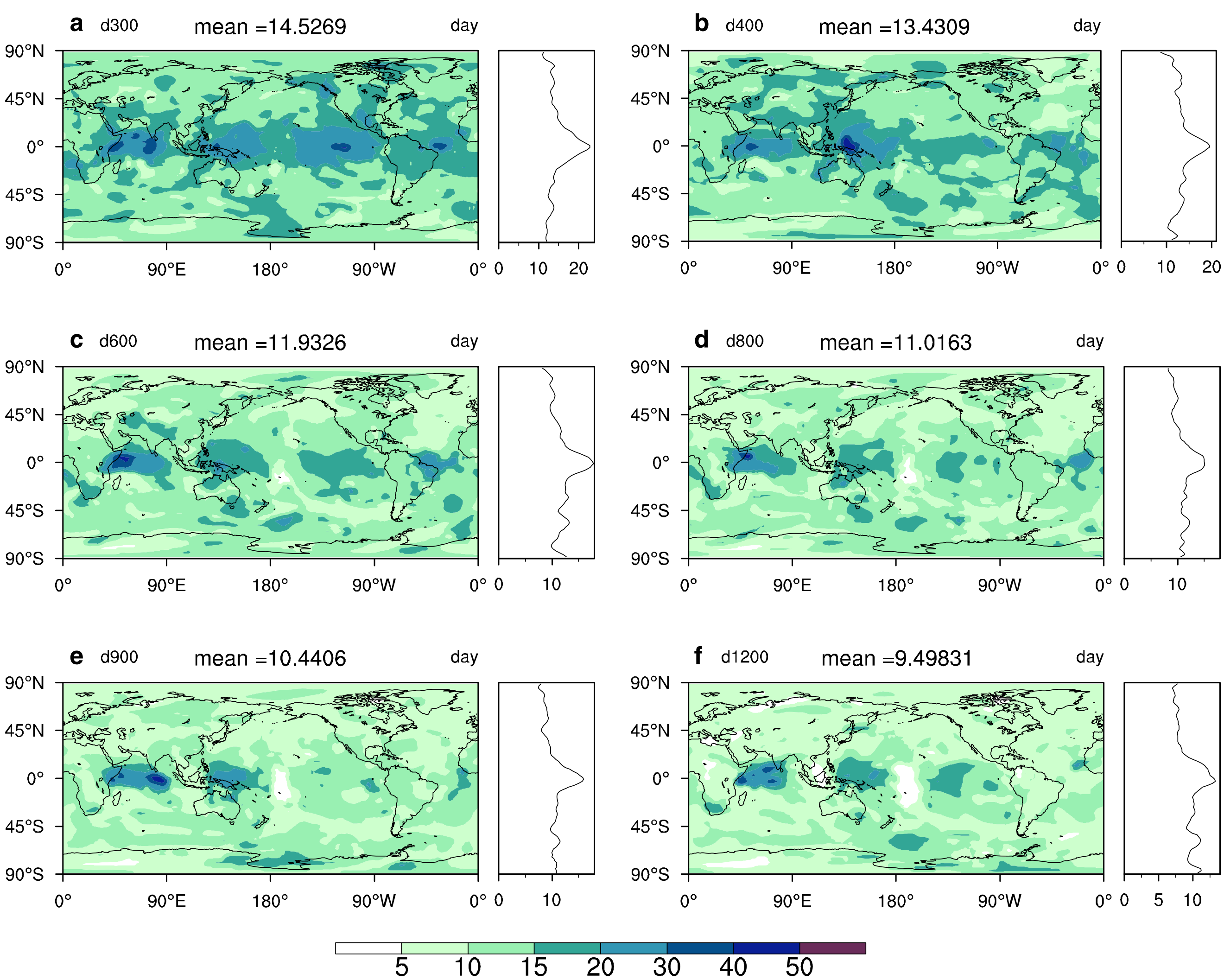

Fig. 9 Like Fig. 8 but for the CTL experiment

can be seen that the high-value areas of the RCT are mainly located in the tropics having four maximum centers over the northern Indian Ocean, western and eastern Pacific Ocean, and tropical Atlantic Ocean. As the increase of the time steps from 300 to 1,200 s, the amplitudes of the RCT over the four maximum centers decrease significantly, especially over the Atlantic Ocean, and the global mean RCTs of the model also reveal decreasing features having values from 13.29 days (Fig. 8a) to 9.58 days (Fig. 8f). The zonal mean RCTs indicate that the global mean RCTs is almost beyond 10 days with the exception over the high latitudes in the NH, and the maximum center notably situates over the tropics with value above 17.5. Moreover, the RCTs over SH is about 2~3 days longer than those over NH, which suggests the RCTs over NH is more sensitive than those over SH.

Without the SST forcing, a similar experiment to the AMIP experiment is made, i.e., the CTL experiment. Corresponding to the CTL experiment, the RCTs distribution of 500 hPa geopotential height is shown in Fig. 9. The high values of the RCTs are also situated over the tropics, having four maximum centers located over the northern Indian Ocean, western and eastern Pacific Ocean, and tropical Atlantic Ocean. As the increase of the time step, the amplitudes of the RCTs and their global mean exhibit evident decrease; this resembles the features in the AMIP experiment. In contrast to the features in Fig. 8, the high-value centers over the northern Indian Ocean and western Pacific Ocean are more stable despite its decrease in amplitude with the time step. The zonal mean RCTs reveal similar features in Fig. 8, except that the discrepancy between the NH and SH weakens. It can be concluded that with SST forcing, the asymmetry of the RCT over SH and NH enhances because of the large span of ocean area and the SST hemispheric contrast between NH and SH.

The result of the CTL-JJA experiment is plotted in Fig. 10. The spatial distribution of the RCTs is irregular comparing to that in Fig. 9. The high-value centers are located in the tropics having similar areas to those in Fig. 9. However, as the increase of the time step, the

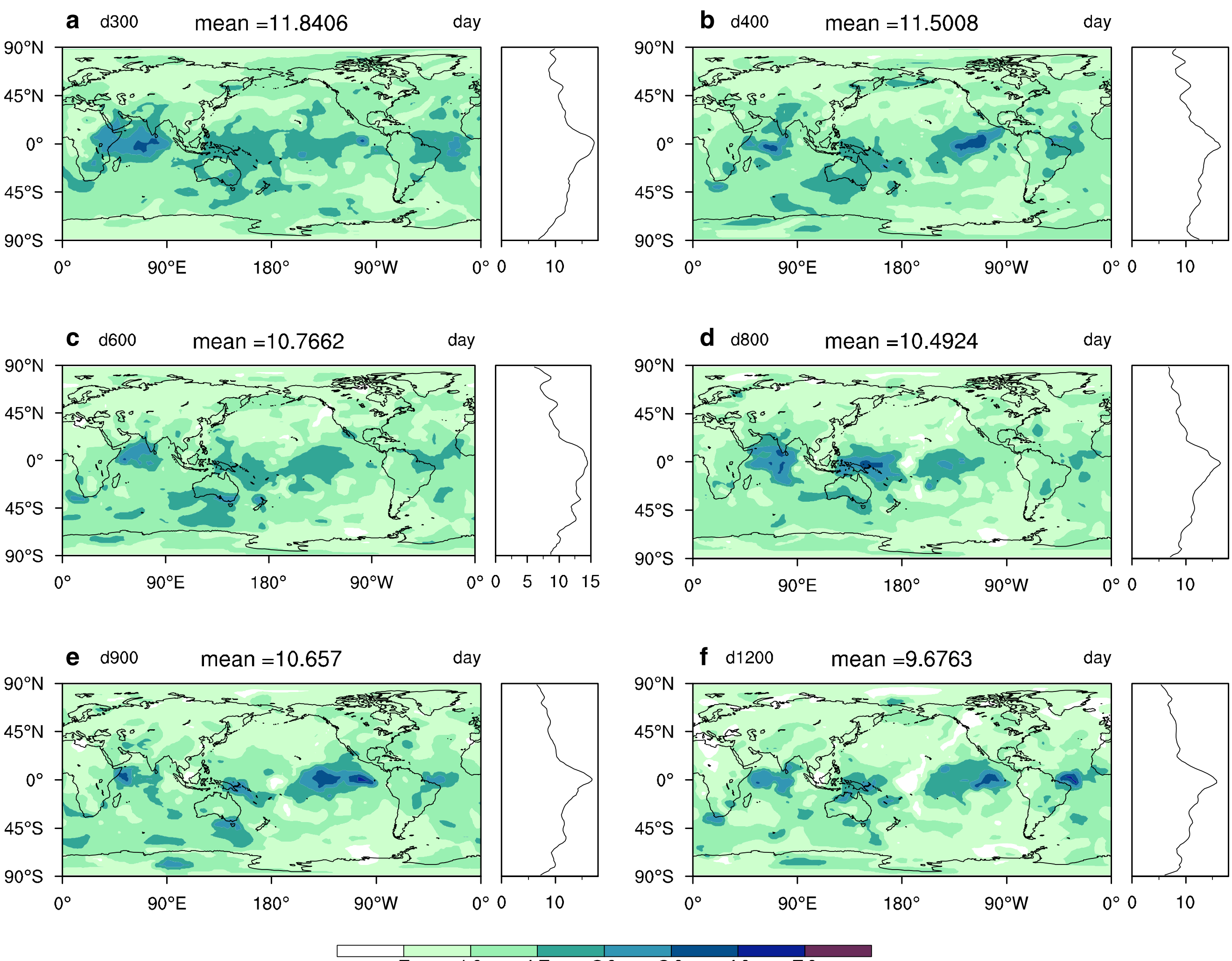

Fig. 10 Like Fig. 8 but for the CTL-JJA experiment

amplitude of the maximum centers decreases over the northern Indian Ocean and western Pacific Ocean but increase over the eastern Pacific Ocean and tropical Atlantic Ocean. The global mean RCTs is about 2 days shorter than those in CTL run, and they decrease more slowly. This indicates the seasonality characteristic of the RCTs, and the error may develop faster in summer than that in winter, but RCTs reaches 9.5 days when the errors saturate (Fig. 10d).

Figure 11 depicts the spatial distribution of RCTs based on the CTL-T106 experiment. We can observe that the RCTs of the high-resolution version model resemble those of low-resolution one, namely that the RCTs have maximum centers over the northern Indian Ocean, western and eastern Pacific Ocean, and tropical Atlantic Ocean and decrease with the increasing of the time step. Comparing to Fig. 9, the RCTs of the high-resolution model are shorter. With respect of the zonal mean of the RCTs, the maximum value in the tropics is longer than that in Fig. 9 and the RCTs reveal evident symmetric features.

We also investigated the vertical distribution of RCTs of the model based on the AMIP experiment. When the integration time step is close to the reference time step (Fig. 12a–c), the high-value areas of the RCT is over the mid/high troposphere and the amplitude can reach about 15–18 days, especially over the tropics. As the time step increases, the RCTs decrease significantly above 300 hPa in the tropics and the low/middle level around 60° N (about 3~6 days), but increase in the high latitudes in the NH (Fig. 12d–f). The RCTs over the low level in the tropics and other regions change a little, and the vertical distribution of the RCTs over polar area reveals barotropical features. These characteristics can also be observed in the CTL experiment (figures not shown).

5 Conclusion and discussion

The present study investigated the PT of the Lorenz system and Chen system using the simple STC method, because the

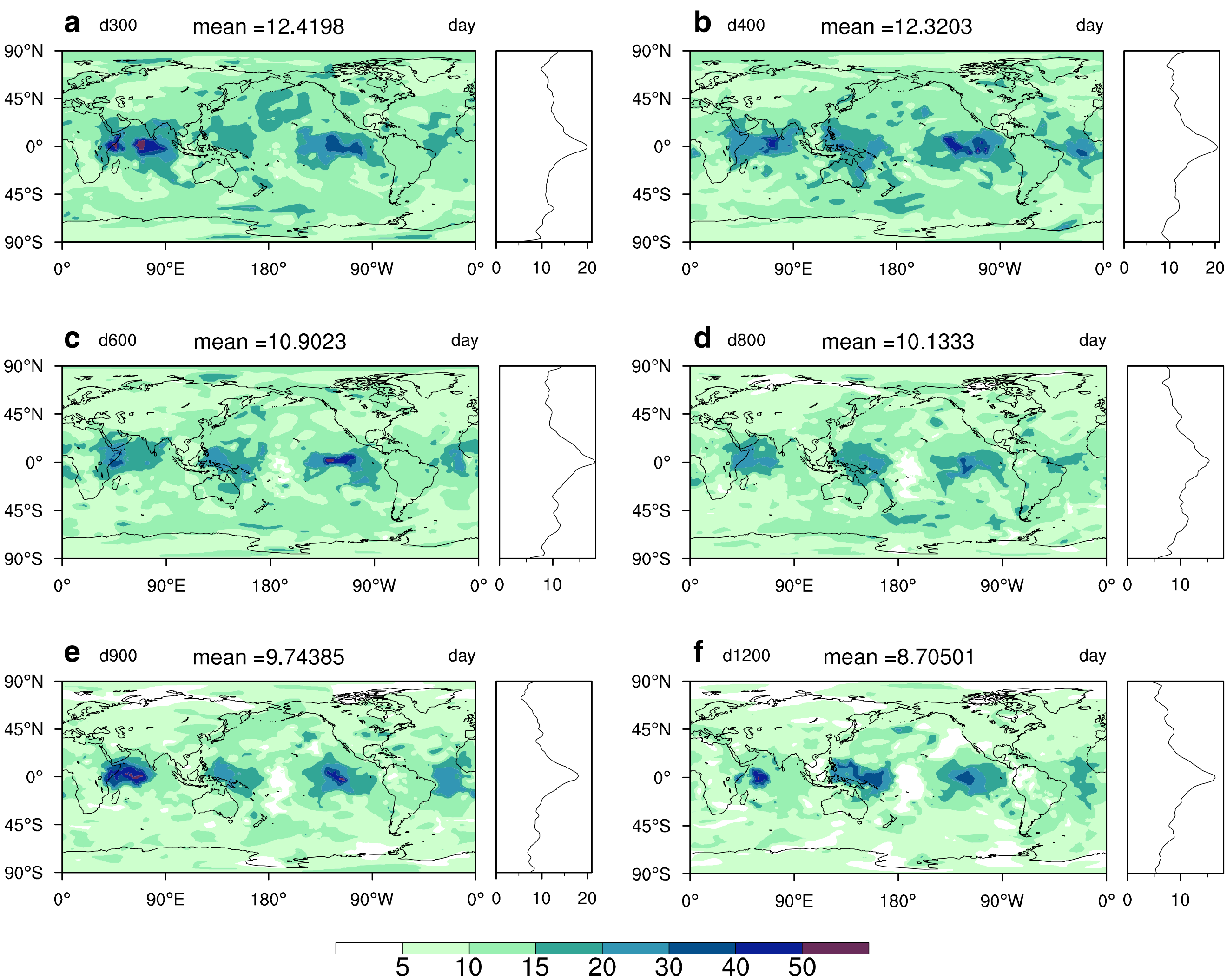

Fig. 11 Like Fig. 8 but for the CTL-T106 experiment

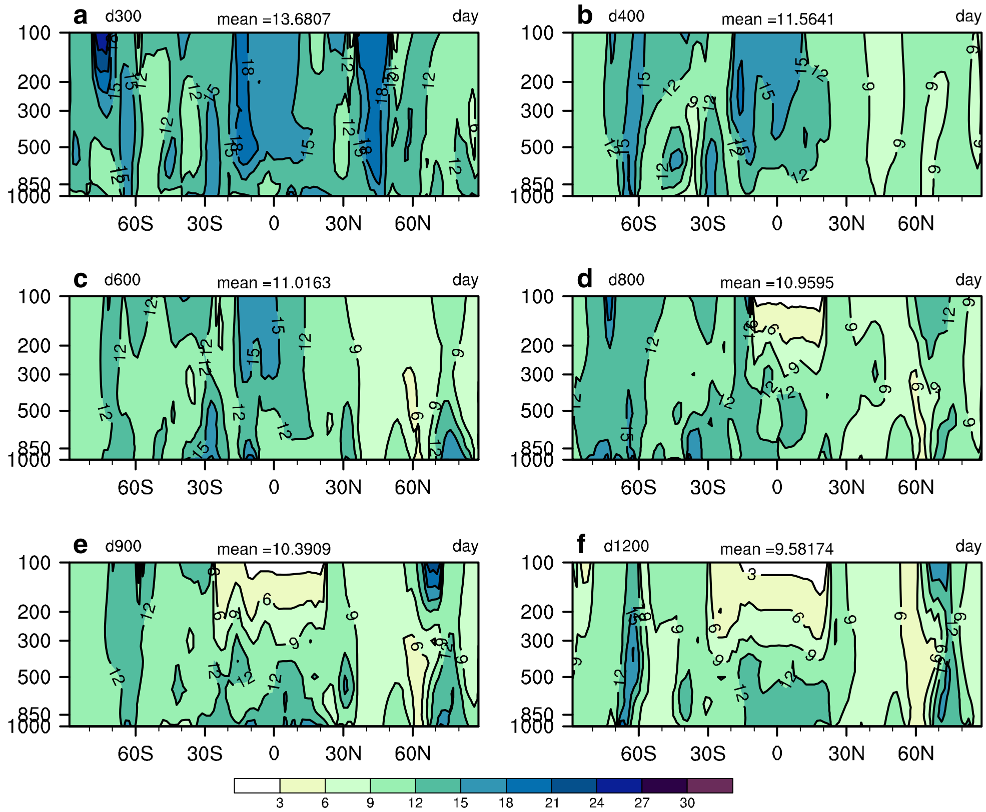

Fig. 12 The vertical distribution of the zonal mean RCTs (unit: day) of the geopotential height based on the AMIP experiment

intrinsic characteristics of these chaotic systems are different from each other, especially their maximum Lyapunov exponents, which bring about different error accumulation and further the PTs. The PTs, T_c−*M* and T_c−*K* diagrams of each chaotic system detected by STC, match well with that by the error limitation method. The result indicates the effectiveness of the STC in studying the PT and RCT.

By using the STC method, taking the geopotential height for example, the RCT of ECHAM5 and potential impact factors such as the integration time step, initial condition, and model's resolution are explored through kinds of numerical experiments. Results indicate that (1) the high-value areas of the RCT are mainly situated in the tropics, and the GMRCT decreases as the time step increases; (2) the ocean forcing can enlarge the difference of the RCT between that of the averaged over SH and NH, which implies the RCT in the NH may be more sensitive to the computation error than that in the SH; (3) the model's RCT also displays significant seasonality showing longer (about 1–2 days) GMRCT in the experiment integrating from winter than that from summer; (4) the RCT of the high-resolution (T106) ECHAM5 shows similar spatial feature to that of low-resolution (T63) ECHAM5, but the GMRCT and hemispheric difference decreases.

In contrast to the studies on the PT of the weather system using the observational data and NLLE method by Ding and Li (2007b), the present work also shows maximum RCTs in the tropics, but the RCTs in present study over the northern and southern Polar Regions are shorter than those in Ding and Li (2007a, b). This suggests the RCT over the Polar Regions is sensitive to the error accumulation, which is contrary to that it should have longer RCT. On this view, it can be concluded the error around the Polar Regions is not well controlled in the model, which is one difficulty point in improving the model's performance.

The STC method is simply based on the statistics and investigates the RCT of numerical models using sequential time series, revealing effectiveness and advantages in easy computing, dynamical clarity, and accuracy. It can be widely used to study not only the error development of dynamic systems but also in the distinct PT of the real climate using the reanalysis datasets, which will be explored in future work.

Acknowledgement This research was jointly supported by the National Basic Research Program of China (2011CB309704) and the National Natural Science Foundation of China (41375112), and the Strategic Priority Research Program of the Chinese Academy of Sciences (XDA05090402), the National Natural Science Foundation of China (41275083 and 91337105).

References

Chen G, Ueta T (1999) Yet another chaotic attractor. Int J Bifurcation Chaos 9:1465–1466

Ding RQ, Li JP (2007a) Nonlinear finite-time Lyapunov exponent and predictability. Phys Lett A 364:396–400

Ding RQ, Li JP (2007b) The temporal–spatial distributions of weather predictability of different variables. Acta Meteorol Sin 67(3):343–354

Ding RQ, Li JP (2012) Relationships between the limit of predictability and initial error in the uncoupled and coupled Lorenz models. Adv Atmos Sci 29:1–11

Eckmann J-P, Ruelle D (1985) Ergodic theory of chaos and strange attractors. Rev Mod Phys 57:617

Li JP, Ding RQ (2011) Temporal–spatial distribution of atmospheric predictability limit by local dynamical analogues. Mon Weather Rev 139:3265–3283

Li JP, Zeng QC, Chou JF (2000) Computational uncertainty principle in nonlinear ordinary differential equations—I. numerical results. Sci China Ser E 43:449–461

Liao SJ (2009) On the reliability of computed chaotic solutions of nonlinear differential equations. Tellus A 61:550–564

Liao S, Wang P (2014) On the mathematically reliable long-term simulation of chaotic solutions of Lorenz equation in the interval [0,10000]. Sci China: Physics, Mechanics and Astronomy. 57(2): 330–335

Lorenz EN (1963) Deterministic nonperiodic flow. J Atmos Sci 20: 130–141

Lorenz EN (1996) Predictability—a problem partly solved. Proc. Seminar on predictability

Oseledec VI (1968) A multiplicative ergodic theorem. Lyapunov characteristic numbers for dynamical systems. Trans Mosc Math Soc 19: 197–231

Roeckner E (2003) The atmospheric general circulation model ECHAM5: part 1: model description. Max-Planck-Institut für Meteorologie

Song Z, Qiao F, Lei X, Wang C (2012) Influence of parallel computational uncertainty on simulations of the coupled general climate model. Geosci Model Dev 5:313–319

Teixeira J, Reynolds CA, Judd K (2007) Time step sensitivity of nonlinear atmospheric models: numerical convergence, truncation error growth, and ensemble design. J Atmos Sci 64:175–189. doi:10.1175/jas3824.1

Wang PF, Huang G, Wang ZZ (2006) Analysis and application of multiple precision computation and round-off error for nonlinear dynamical systems. Adv Atmos Sci 23:758–766

Wang P, Jianping L, Lei G (2009) Understanding and application of the decay theory of initial condition effect in numerical climate simulation studies. Acta Meteorol Sin 67:218–226

Wang PF, Li JP, Li Q (2012) Computational uncertainty and the application of a high-performance multiple precision scheme to obtaining the correct reference solution of Lorenz equations. Numer Algorithm 59:147–159

Wolf A, Swift JB, Swinney HL, Vastano JA (1985) Determining Lyapunov exponents from a time series. Phys D: Nonlinear Phenom 16:285–317

Yoden S, Nomura M (1993) Finite-time Lyapunov stability analysis and its application to atmospheric predictability. J Atmos Sci 50: 1531–1543